CHIN. PHYS. LETT. Vol. 35, No. 11 (2018) 113201

# Simulation of Intermediate State Absorption Enhancement in Rare-Earth Ions by Polarization Modulated Femtosecond Laser Field *

Wen-Jing Cheng(程文静)**, Shi-Hua Zhao(赵世华)

*School of Electrical & Electronic Information, Shangqiu Normal University, Shangqiu 476000*

(Received 14 August 2018)

*We extend the third perturbation theory to study the polarization control behavior of the intermediate state absorption in $Nd^{3+}$ ions. The results show that coherent interference can occur between the single-photon and three-photon excitation pathways, and depends on the central frequency of the femtosecond laser field. Moreover, single-photon and three-photon absorptions have different polarization control efficiencies, and the relative weight of three-photon absorption in the whole excitation processes can increase with increasing the laser intensity. Therefore, the enhancement or suppression of the intermediate state absorption can be realized and manipulated by properly designing the intensity and central frequency of the polarization modulated femtosecond laser field. This research can not only enrich theoretical research methods for the up-conversion luminescence manipulation of rare-earth ions, but also can provide a clear physical picture for understanding and controlling multi-photon absorption in a multiple energy level system.*

*PACS: 32.80.Qk, 32.80.Wr* DOI: 10.1088/0256-307X/35/11/113201

The up-conversion luminescence of rare-earth ions is a nonlinear optical phenomenon, which can convert low frequency photons to high frequency emissions by absorbing two or more photons. The up-conversion luminescence of rare-earth ions exhibits attracting optical properties, such as photo-stability, narrow spectrum, near infrared excitation, large Stokes shift and long luminescence lifetime.[1,2] At present, rare-earth doped materials have attracted much attention and have been widely applied in laser sources, fiber-optic communications, light-emitting diodes, biolabeling and biomedical sensing.[3–7] With the development of the science and technology, a shaped pulse with an almost arbitrary temporal distribution can be obtained by controlling the spectral phase, amplitude and polarization of the femtosecond laser field, which can provide new technology and ideas for tuning the up-conversion luminescence of rare-earth ions. So far, various schemes have been proposed to manipulate the multi-photon absorption of rare-earth ions. For example, the $\pi$ or square phase modulation has been used to enhance or suppress the single-photon and two-photon fluorescence of $Er^{3+}$ ions.[8,9] The up-conversion fluorescence in $Dy^{3+}$ or $Er^{3+}$ ions have been effectively manipulated by the laser polarization and phase modulation.[10,11] The red and green up-conversion luminescence in $Er^{3+}$-doped nanocrystals can be tuned by the square phase modulation.[12] Moreover, the polarization control efficiency in $Dy^{3+}$-doped glass sample can be manipulated by the femtosecond spectral frequency modulation.[13] Similarly, the multi-mode correlation and squeezing of parametrically amplified multi-wave mixing in $Pr^{3+}$:$Y_2SiO_5$ or diamond nitrogen-vacancy (NV) centers can be controlled by multi-parameters, including the power, polarization, and the frequency detuning of the laser field.[14–17]

The research mentioned above has mainly focused on the multi-photon absorption modulation of the goal state in a weak femtosecond laser field, and has neglected the effects of the higher excited states.[8–13] However, under an intermediate femtosecond laser field excitation, the higher excited states are always involved owing to the higher-order nonlinear effects, which will further influence the target state absorption. Therefore, it becomes necessary to consider the influence of the higher excited state on the target state absorption in rare-earth ions. In this Letter, we further extend the third-order perturbation theory to study the polarization control modulation of the intermediate state absorption in $Nd^{3+}$ ions. We show that the intermediate state absorptions result from the single-photon and three-photon processes, and the constructive or destructive interference between them depends on the central frequency of the femtosecond laser field. Moreover, the polarization control efficiency of three-photon absorption is higher than that of single-photon absorption. The occurrence of three-photon absorption in all of the excitation processes increases with the laser intensity, and the polarization control efficiency of the intermediate state absorption can be manipulated by the laser intensity.

To study the intermediate state absorption in multiple energy level systems, we establish a three-level energy model in $Nd^{3+}$ ions. As shown in Fig. 1(a), the ground state $|g\rangle$, intermediate state $|i\rangle$ and final state $|f\rangle$ represent the three states $^4I_{9/2}$, $^4F_{3/2}$ and $^2P_{1/2}$ in $Nd^{3+}$ ions, respectively. When the $Nd^{3+}$

*Supported by the National Natural Science Foundation of China under Grant Nos 51132004, 11474096, 11604199, U1704145 and 11747101, the Science and Technology Commission of Shanghai Municipality under Grant No 14JC1401500, the Henan Provincial Natural Science Foundation of China under Grant No 182102210117, and the Higher Education Key Program of He'nan Province of China under Grant Nos 17A140025 and 16A140030.

**Corresponding author. Email: 0110wenjing@163.com

© 2018 Chinese Physical Society and IOP Publishing Ltd

ions are excited by the femtosecond laser field, the intermediate state $|i\rangle$ can be populated by two excitation processes, that is, single-photon and three-photon absorptions. Obviously, in the single-photon absorption process, the ground state population is directly pumped to the intermediate state $|i\rangle$ by absorbing one photon with the transition frequency of $|g\rangle \to |i\rangle$. However, for the three-photon absorption process, the transition pathways include the resonant Raman parts through the ground state $|g\rangle$ and the final state $|f\rangle$, and the three photons involve two absorbed photons and one emitted photon, which is different from the upwards excitation three-photon process that absorbs photons one by one. To clearly describe all of the excitation processes, the digital symbols of ①, ②, and ③ were used to label the transition sequence of the single-photon and three-photon pathways.

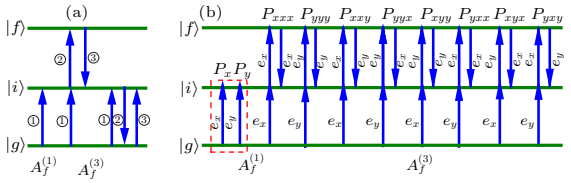


**Fig. 1.** (Color online) (a) The single-photon and three-photon transition processes in $Nd^{3+}$ ions. (b) The possible excitation pathways of the single-photon and three-photon transition processes under a polarization modulated femtosecond laser field.

Here we construct a third-order perturbation theory to describe single-photon and three-photon absorptions, which includes the first-order and third-order perturbation terms, that is, $A_i^{(1)}$ and $A_i^{(3)}$. The intermediate state transition probability $P_i$ can be expressed as

$$P_i \propto \int_{-\infty}^{+\infty} d\omega_{\rm ig} A_{\rm abs}(\omega_{\rm ig}) |A_i^{(1)} + A_i^{(3)}|^2. \tag{1}$$

The first-order term $A_i^{(1)}$ is the single-photon transition pathway from ground-to-intermediate state ($|g\rangle \to |i\rangle$), and can be described as

$$A_i^{(1)} = \frac{i|E_0|}{\hbar}[i\pi\mu_{\rm ig}\overline{E}(\omega_{\rm ig})]. \tag{2}$$

Meanwhile, the third-order term $A_i^{(3)}$ can be divided into four parts: on-on resonant term $A_i^{(3){\rm on-on}}$, on-near resonant term $A_i^{(3){\rm on-near}}$, near-on resonant term $A_i^{(3){\rm near-on}}$, and near-near resonant term $A_i^{(3){\rm near-near}}$. Thus the third-order term $A_i^{(3)}$ can be expressed as

$$\begin{aligned} A_i^{(3)} = {} & A_i^{(3){\rm on-on}} + A_i^{(3){\rm on-near}} \\ & + A_i^{(3){\rm near-on}} + A_i^{(3){\rm near-near}}. \end{aligned} \tag{3}$$

In the on-on resonant three-photon process, the ground state population is first pumped to the intermediate state $|i\rangle$ by absorbing one photon with the transition frequency of $|g\rangle \to |i\rangle$, then pumped to the intermediate state $|i\rangle$ through the ground state $|g\rangle$ by emitting and absorbing one photon with the transition frequency of $|g\rangle \to |i\rangle$ or through the final state $|f\rangle$ by absorbing and emitting one photon with the transition frequency of $|i\rangle \to |f\rangle$. For the on-near resonant three-photon process, the ground state population is first pumped to the intermediate state $|i\rangle$, then pumped to the intermediate state $|i\rangle$ without going through the two states $|f\rangle$ or $|g\rangle$ by absorbing and emitting one photon. Thus the transition probability amplitude of the on-on resonant $A_i^{(3){\rm on-on}}$ and on-near resonant $A_i^{(3){\rm on-near}}$ terms can be written as[18–20]

$$\begin{aligned} A_i^{(3){\rm on-on}} = {} & \frac{i|E_0|^3}{\hbar^3}\Big\{ i\pi\mu_{\rm ig}\overline{E}(\omega_{\rm ig})[i\pi|\mu_{\rm ig}|^2 \\ & \cdot \int_{-\infty}^{+\infty} d\omega_{\rm ig} A_{\rm abs}(\omega_{\rm ig})\overline{E}^*(\omega_{\rm ig})\overline{E}(\omega_{\rm ig}) + i\pi|\mu_{\rm fi}|^2 \\ & \cdot \int_{-\infty}^{+\infty} d\omega_{\rm fi} A_{\rm abs}(\omega_{\rm fi})\overline{E}^*(\omega_{\rm fi})\overline{E}(\omega_{\rm fi})]\Big\}, \end{aligned} \tag{4}$$

$$\begin{aligned} A_i^{(3){\rm on-near}} = {} & \frac{i|E_0|^3}{\hbar^3}[i\pi\mu_{\rm ig}\overline{E}(\omega_{\rm ig})] \\ & \cdot \Big\{ -\wp\int_{-\infty}^{\infty} d\delta' \Big[ \frac{|\mu_{\rm ig}|^2\overline{E}^*(\omega_{\rm ig}-\delta')\overline{E}(\omega_{\rm ig}-\delta')}{\delta'} \\ & + \frac{|\mu_{\rm fi}|^2\overline{E}^*(\omega_{\rm fi}-\delta')\overline{E}(\omega_{\rm fi}-\delta')}{\delta'}\Big]\Big\}. \end{aligned} \tag{5}$$

In the near-on resonant three-photon process, the population in the ground state $|g\rangle$ is pumped to the ground state $|g\rangle$ or the final state $|f\rangle$ without the intermediate state $|i\rangle$, then pumped to the intermediate state $|i\rangle$ by absorbing one photon with the transition frequency of $|g\rangle \to |i\rangle$ or emitting one photon with the transition frequency of $|i\rangle \to |f\rangle$. For the near-near resonant three-photon process, the population in the ground state $|g\rangle$ is directly pumped to the intermediate state $|i\rangle$ without the three states $|g\rangle$, $|i\rangle$ and $|f\rangle$ by absorbing two photons and emitting one photon. The transition probability amplitude of the near-on $A_i^{(3){\rm near-on}}$ and near-near resonant $A_i^{(3){\rm near-near}}$ terms can be approximated as[18–20]

$$\begin{aligned} A_i^{(3){\rm near-on}} = {} & \frac{i|E_0|^3}{\hbar^3}\Big\{ -\wp\int_{-\infty}^{\infty} d\delta \frac{\mu_{\rm ig}\overline{E}(\omega_{\rm ig}-\delta)}{\delta} \\ & \cdot [i\pi|\mu_{\rm ig}|^2 \int_{-\infty}^{+\infty} d\omega_{\rm ig} A_{\rm abs}(\omega_{\rm ig})\overline{E}^*(\omega_{\rm ig}-\delta)\overline{E}(\omega_{\rm ig}) \\ & + i\pi|\mu_{\rm fi}|^2 \int_{-\infty}^{+\infty} d\omega_{\rm fi} A_{\rm abs}(\omega_{\rm fi})\overline{E}(\omega_{\rm fi}+\delta)\overline{E}^*(\omega_{\rm fi})]\Big\}, \end{aligned} \tag{6}$$

$$\begin{aligned} A_i^{(3){\rm near-near}} = {} & \frac{i|E_0|^3}{\hbar^3}\Big\{ -\wp\int_{-\infty}^{\infty} d\delta \frac{\mu_{\rm ig}\overline{E}(\omega_{\rm ig}-\delta)}{\delta} \\ & \cdot \Big[ -\wp\int_{-\infty}^{\infty} d\delta' [|\mu_{\rm ig}|^2\overline{E}^*(\omega_{\rm ig}-\delta-\delta')\overline{E}(\omega_{\rm ig}-\delta') \\ & + |\mu_{\rm fi}|^2\overline{E}(\omega_{\rm fi}+\delta-\delta')\overline{E}^*(\omega_{\rm fi}-\delta')]/\delta'\Big]\Big\}, \end{aligned} \tag{7}$$

where $\wp$ is the Cauchy principal value, $\omega_{\rm ig}$ and $\omega_{\rm fi}$ are the transition frequencies of $|g\rangle \to |i\rangle$ and $|i\rangle \to |f\rangle$,

$\mu_{ig}$ and $\mu_{fi}$ are the corresponding dipole moment matrix elements, $A(\omega_{ig})$ and $A(\omega_{fi})$ are the absorption line-shape functions of intermediate state $|i\rangle$ and final state $|f\rangle$, the normalized spectral field $\overline{E}(\omega) = E(\omega)/|E_0|$ is used to represent the laser field shape, $E(\omega)$ indicates the spectral amplitude at the frequency $\omega$, and $E_0$ is the maximal spectral amplitude. In our theoretical simulation, the transition frequencies of $\omega_{ig}$ and $\omega_{fi}$ are 11280 and 11860 $\mathrm{cm}^{-1}$, the state absorption bandwidths (FWHMs) are both 100 $\mathrm{cm}^{-1}$, and the ratio of $\mu_{ig}$ and $\mu_{fi}$ is set as 0.01:0.01. The femtosecond laser field is of a Gaussian shape with the central frequency of 11280 $\mathrm{cm}^{-1}$ and the pulse duration of 50 fs.

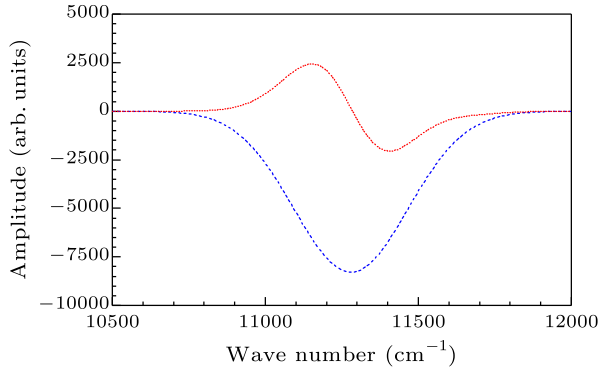


**Fig. 2.** (Color online) The transition probability amplitude real part of the singe-photon (blue dashed line) and three-photon (red dotted line) by varying the central frequency with the femtosecond laser field intensity of $1 \times 10^{13}$ W/cm$^2$.

For the transform-limited (TL) femtosecond laser field (i.e., $\phi(\omega) = 0$), the transition probability amplitudes of $A_i^{(1)}$, $A_i^{(3)\mathrm{on-near}}$ and $A_i^{(3)\mathrm{near-on}}$ are real quantities (see Eqs. (2), (5) and (6)), while those of $A_i^{(3)\mathrm{on-on}}$ and $A_i^{(3)\mathrm{near-near}}$ are imaginary quantities (see Eqs. (4) and (7)). Clearly, destructive or constructive interference can occur between the first-order term $A_i^{(1)}$ and the third-order terms $A_i^{(3)\mathrm{on-near}}$ and $A_i^{(3)\mathrm{near-on}}$. Moreover, $\delta$ is the detuning from the intermediate state $|i\rangle$ (see Eq. (6)), $\delta'$ is the detuning from the ground state $|g\rangle$ or final state $|f\rangle$ (see Eq. (5)). The sign of the near-on resonant term $A_i^{(3)\mathrm{near-on}}$ and the on-near resonant term $A_i^{(3)\mathrm{on-near}}$ can be changed by varying the central frequency of the femtosecond laser field. When the signs of single-photon absorption $A_f^{(1)}$ and that of three-photon absorption $(A_f^{(3)\mathrm{near-on}} + A_f^{(3)\mathrm{on-near}})$ are identical, constructive interference can occur between the single-photon and three-photon excitation pathways, and vice-versa. Furthermore, one can see that the first-order term $A_f^{(1)}$ is proportional to $|E_0|$ (see Eq. (2)), while the third-order term $A_f^{(3)}$ is proportional to $|E_0|^3$ (see Eqs. (4)–(7)). Therefore, the contribution of three-photon absorption to all of the excitation processes can increase with the laser intensity. Considering the various experimental systems with different laser parameters, we will further analyze the effects of the laser intensity and central frequency on the intermediate state absorption in the following.

To illustrate the influence of the femtosecond laser central frequency on the coherent interference between the single-photon and three-photon transition pathways, we calculate the transition probability amplitude real part of the single-photon and three-photon parts (i.e., $A_i^{(1)}$ and $(A_i^{(3)\mathrm{on-near}} + A_i^{(3)\mathrm{near-on}})$) by varying the central frequency with the laser intensity of $1 \times 10^{13}$ W/cm$^2$, and the theoretical results are shown in Fig. 2. When the central frequency is changed from 10500 to 11280 $\mathrm{cm}^{-1}$, the signs between the single-photon (blue dashed line) and three-photon parts (red dotted line) are opposite, which can induce destructive interference between their excitation pathways. However, when the central frequency changes from 11280 to 12000 $\mathrm{cm}^{-1}$, the sign of the single-photon part will be identical to that of the three-photon part, which can create a constructive interference. Therefore, constructive or destructive interference between single-photon and three-photon excitation pathways can be artificially modulated by varying the laser central frequency, which further affects the intermediate state absorption.

The femtosecond laser polarization technique is quite a simple and well-established method to control multi-photon absorption. Here a polarization modulated femtosecond laser field is applied as the excitation source in our theoretical simulation. Usually, the polarization modulation femtosecond laser field can be produced by a quarter wave ($\lambda/4$) plate, and its polarization status in the space can be decomposed into two orthogonal directions, that is, $\hat{\boldsymbol{e}}_x$ and $\hat{\boldsymbol{e}}_y$,

$$\boldsymbol{E}_{\lambda/4}(t) = \cos(\theta)E(t)\hat{\boldsymbol{e}}_x + \sin(\theta)E(t)\hat{\boldsymbol{e}}_y, \qquad (8)$$

where $\theta$ is the angle between the input laser polarization direction and the optical axis of the quarter wave plate. It is clear that the output laser field is of linear polarization for $\theta = m\pi/2$ ($m = 0, 1, 2\ldots$), circular polarization for $\theta = (2m+1)\pi/4$, and elliptical polarization for other angles of $\theta$. Figure 1(b) shows the possible excitation pathways for the single-photon and one for on-on resonant three-photon processes by the polarization modulated femtosecond laser field. As can be seen, in the single-photon transition process, the photon can come from different polarization directions (i.e., $\hat{\boldsymbol{e}}_x$ and $\hat{\boldsymbol{e}}_y$). For the three-photon process, the on-resonant photon can come from different polarization directions, while the near-resonant photon should come from the same polarization direction. Therefore, for the three-photon absorption processes, the polarization modulated femtosecond laser field can induce several different excitation pathways. The transition pathways of the on-on resonant term $A^{(3)\mathrm{on-on}}$ have multiple polarization combination ways (i.e., $\hat{\boldsymbol{e}}_x\hat{\boldsymbol{e}}_x\hat{\boldsymbol{e}}_x$, $\hat{\boldsymbol{e}}_y\hat{\boldsymbol{e}}_y\hat{\boldsymbol{e}}_y$, $\hat{\boldsymbol{e}}_x\hat{\boldsymbol{e}}_y\hat{\boldsymbol{e}}_y$, $\hat{\boldsymbol{e}}_y\hat{\boldsymbol{e}}_x\hat{\boldsymbol{e}}_x$, $\hat{\boldsymbol{e}}_x\hat{\boldsymbol{e}}_x\hat{\boldsymbol{e}}_y$, $\hat{\boldsymbol{e}}_y\hat{\boldsymbol{e}}_y\hat{\boldsymbol{e}}_x$, $\hat{\boldsymbol{e}}_y\hat{\boldsymbol{e}}_x\hat{\boldsymbol{e}}_y$, and $\hat{\boldsymbol{e}}_x\hat{\boldsymbol{e}}_y\hat{\boldsymbol{e}}_x$), as shown in

Fig. 1(b), but the photons for the near-near resonant term $A^{(3)\mathrm{near-near}}$ should come from the same polarization direction (i.e., $\hat{\boldsymbol{e}}_x\hat{\boldsymbol{e}}_x\hat{\boldsymbol{e}}_x$ and $\hat{\boldsymbol{e}}_y\hat{\boldsymbol{e}}_y\hat{\boldsymbol{e}}_y$). Similarly, the polarization combinations of the on-near resonant term $A_f^{(3)\mathrm{on-near}}$ are $\hat{\boldsymbol{e}}_x\hat{\boldsymbol{e}}_x\hat{\boldsymbol{e}}_x$, $\hat{\boldsymbol{e}}_y\hat{\boldsymbol{e}}_y\hat{\boldsymbol{e}}_y$, $\hat{\boldsymbol{e}}_x\hat{\boldsymbol{e}}_y\hat{\boldsymbol{e}}_y$, and $\hat{\boldsymbol{e}}_y\hat{\boldsymbol{e}}_x\hat{\boldsymbol{e}}_x$, and those of the near-on resonant term $A_f^{(3)\mathrm{near-on}}$ are $\hat{\boldsymbol{e}}_x\hat{\boldsymbol{e}}_x\hat{\boldsymbol{e}}_x$, $\hat{\boldsymbol{e}}_y\hat{\boldsymbol{e}}_y\hat{\boldsymbol{e}}_y$, $\hat{\boldsymbol{e}}_x\hat{\boldsymbol{e}}_x\hat{\boldsymbol{e}}_y$, and $\hat{\boldsymbol{e}}_y\hat{\boldsymbol{e}}_y\hat{\boldsymbol{e}}_x$. The transition probability amplitudes of these different excitation pathways can be written as

$$f_x = \cos\varphi \times A_i^{(1)}, \tag{9}$$

$$f_{xxx} = \cos^3\varphi \times (A_i^{(3)\mathrm{on-on}} + A_i^{(3)\mathrm{on-near}} + A_i^{(3)\mathrm{near-on}} + A_i^{(3)\mathrm{near-near}}), \tag{10}$$

$$f_y = \sin\varphi \times A_i^{(1)}, \tag{11}$$

$$f_{yyy} = \sin^3\varphi \times (A_i^{(3)\mathrm{on-on}} + A_i^{(3)\mathrm{on-near}} + A_i^{(3)\mathrm{near-on}} + A_i^{(3)\mathrm{near-near}}), \tag{12}$$

$$f_{xxy} = \sin^2\varphi\cos\varphi \times (A_i^{(3)\mathrm{on-on}} + A_i^{(3)\mathrm{near-on}}), \tag{13}$$

$$f_{yyx} = \cos^2\varphi\sin\varphi \times (A_i^{(3)\mathrm{on-on}} + A_i^{(3)\mathrm{near-on}}), \tag{14}$$

$$f_{xyy} = \cos\varphi\sin^2\varphi \times (A_i^{(3)\mathrm{on-on}} + A_i^{(3)\mathrm{on-near}}), \tag{15}$$

$$f_{yxx} = \sin\varphi\cos^2\varphi \times (A_i^{(3)\mathrm{on-on}} + A_i^{(3)\mathrm{on-near}}), \tag{16}$$

$$f_{xyx} = \sin\varphi\cos^2\varphi \times A_i^{(3)\mathrm{on-on}}, \tag{17}$$

$$f_{yxy} = \sin^2\varphi\cos\varphi \times A_i^{(3)\mathrm{on-on}}. \tag{18}$$

One can see that all the photons in Eqs. (9) and (10) (or Eqs. (11) and (12)) come from the same horizontal polarization direction (or the perpendicular polarization direction), which means that coherent interference of these excitation pathways can occur. Therefore, the total transition probability $P_i$ of the intermediate states can be written as

$$P_i = \int_{-\infty}^{+\infty} d\omega_{\mathrm{ig}} A(\omega_{\mathrm{ig}})[|f_x + f_{xxx}|^2 + |f_y + f_{yyy}|^2 + |f_{xxy}|^2 + |f_{yyx}|^2 + |f_{xyy}|^2 + |f_{yxx}|^2 + |f_{xyx}|^2 + |f_{yxy}|^2], \tag{19}$$

where the total transition probability $P_i$ of the intermediate state includes the contributions of both single-photon and three-photon absorption, and constructive or destructive interference can occur between the single-photon and three-photon excitation pathways (i.e., $|f_x + f_{xxx}|^2$ and $|f_y + f_{yyy}|^2$). Meanwhile, the single-photon and three-photon transition probabilities can also be expressed as

$$P_1 = \int_{-\infty}^{+\infty} d\omega_{\mathrm{ig}} A(\omega_{\mathrm{ig}})[|f_x|^2 + |f_y|^2], \tag{20}$$

$$P_3 = \int_{-\infty}^{+\infty} d\omega_{\mathrm{ig}} A(\omega_{\mathrm{ig}})[|f_{xxx}|^2 + |f_{yyy}|^2 + |f_{xxy}|^2 + |f_{yyx}|^2 + |f_{xyy}|^2 + |f_{yxx}|^2 + |f_{xyx}|^2 + |f_{yxy}|^2]. \tag{21}$$

As can be seen in Eqs. (20) and (21), the single photon transition probability $P_1$ is constant and independent of the rotation angle $\theta$ of the $\lambda/4$ wave plate, whereas the three-photon transition probability $P_3$ is correlated with the rotation angle $\theta$ of the $\lambda/4$ wave plate. To individually observe the polarization control behaviors of single-photon and three-photon absorption, we calculate the TL-normalized single-photon and three-photon transition probability (based on Eqs. (20) and (21)) by varying the rotation angle $\theta$ of the $\lambda/4$ wave plate with a central frequency of $11570\,\mathrm{cm}^{-1}$ and the laser intensity of $1\times10^{13}\,\mathrm{W/cm}^2$. The theoretical results are shown in Fig. 3, where all the data are normalized by the TL femtosecond pulse excitation. As can be seen, when the laser polarization changes from linear through elliptical to circular, the TL-normalized single-photon transition probability $P_1$ (blue dashed line) is constant and independent of the rotation angle $\theta$ of the $\lambda/4$ wave plate. However, the TL-normalized three-photon transition probability $P_3$ (red dotted line) is correlated with the rotation angle $\theta$ of the $\lambda/4$ wave plate, and reaches a maximal value for $\theta = m\pi/2$ ($m = 0, 1, 2\ldots$) and minimal value for $\theta = (2m+1)\pi/4$. Moreover, the single-photon and three-photon absorptions exhibit different polarization control efficiencies, and the polarization control efficiency of single-photon absorption is 0%, while that of three-photon absorption can be up to 40%. Here the polarization control efficiency is defined by the function $\eta = 1 - I^{\min}/I^{\max}$, where $I^{\min}$ and $I^{\max}$ are the minimum and maximum populations of the intermediate state.

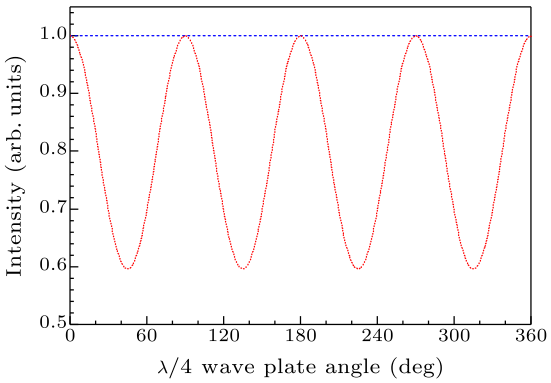


**Fig. 3.** (Color online) The TL-normalized single-photon (blue dashed line) and three-photon transition probability (red dotted line) by varying the rotation angle $\theta$ of the $\lambda/4$ wave plate with the central frequency of $11570\,\mathrm{cm}^{-1}$ and the laser intensity of $1\times10^{13}\,\mathrm{W/cm}^2$.

To study the effects of laser intensity on the polarization control behaviors of the intermediate state absorption, we show the TL-normalized intermediate state absorption by varying the rotation angle $\theta$ of the $\lambda/4$ wave plate under the laser intensities of $1\times10^{12}$ (blue dotted lines), $5\times10^{12}$ (red dashed lines), and $1\times10^{13}\,\mathrm{W/cm}^2$ (green solid lines) with the laser central frequency of $11160\,\mathrm{cm}^{-1}$ in Fig. 4(a) and $11400\,\mathrm{cm}^{-1}$ in Fig. 4(b). All the traces are normalized by the intermediate state absorption induced by the TL pulse. As can be seen in Fig. 4(a), the TL-

normalized intermediate state absorption can be effectively enhanced by the circular polarization under a laser intensity of $1 \times 10^{13}\,\mathrm{W/cm^2}$. These observations can be well explained as follows: single-photon absorption is constant, while three-photon absorption can reach a maximal value for linear polarization and minimal value for circular polarization. Moreover, the contribution from three-photon absorption to all of the excitation processes will increase with the laser intensity. For the central frequency of $11160\,\mathrm{cm^{-1}}$, destructive interference can occur between the single-photon and three-photon excitation pathways, which results in an enhancement of the TL-normalized intermediate state absorption for the circular polarization. Moreover, as shown in Fig. 4(b), with the increase of the laser intensity for the central frequency $11400\,\mathrm{cm^{-1}}$, the TL-normalized intermediate state absorption is effectively suppressed by the circular polarization. Obviously, these observations can be attributed to the constructive interference between the single-photon and three-photon transition pathways. Therefore, the contribution from three-photon part to all of the excitation processes depends on the laser intensity, and the TL-normalized intermediate state absorption and polarization control efficiency can be modulated by selecting an appropriate laser intensity and central frequency.

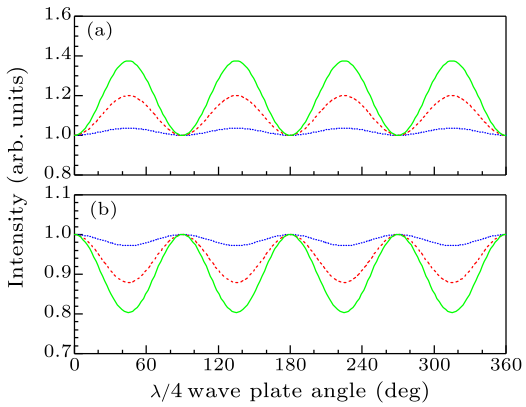


**Fig. 4.** (Color online) The TL-normalized intermediate state absorption by varying the rotation angle $\theta$ of the $\lambda/4$ wave plate under the laser intensities of $1\times10^{12}$ (blue dotted lines), $5\times10^{12}$ (red dashed lines), and $1\times10^{13}\,\mathrm{W/cm^2}$ (green solid lines) with the laser central frequencies of 11160 (a) and $11400\,\mathrm{cm^{-1}}$ (b).

In conclusion, we have constructed a third-order perturbation theory to study the polarization modulation of the intermediate state absorption in $Nd^{3+}$ ions. The intermediate state absorption includes the contributions from both the single-photon and three-photon absorption, and the constructive or destructive interference between them depends on the central frequency of the femtosecond laser field. Moreover, the single-photon and three-photon absorption have different polarization control efficiencies, and the relative weight of three-photon absorption in the whole excitation processes can increase with the laser intensity. Therefore, the enhancement or suppression of the intermediate state absorption can be realized by properly designing the intensity and central frequency of the polarization modulated femtosecond laser field. These theoretical results can provide a clear physical picture for understanding and controlling the multi-photon absorption processes in rare-earth ions, which can enrich the theoretical research methods and provide theoretical guidance for the related experimental works.

## References

[1] Auzel F 2004 *Chem. Rev.* **104** 139
[2] Wang F and Liu X G 2009 *Chem. Soc. Rev.* **38** 976
[3] Wintner E, Sorokin E and Sorokina I T 2001 *Laser Phys.* **11** 1193
[4] Zhou P, Wang X, Ma Y, Lü H and Liu Z J 2012 *Laser Phys.* **22** 1744
[5] Downing E, Hesselink L, Ralston J and Macfarlane R 1996 *Science* **273** 1185
[6] Haase M and Schäfer H 2011 *Angew. Chem. Int. Ed.* **50** 5808
[7] Wolska E, Kaszewski J, Kiełbik P, Grzyb J, Godlewski M M and Godlewski M 2014 *Opt. Mater.* **36** 1655
[8] Zhang S A, Lu C H, Jia T Q, Qiu J R and Sun Z R 2013 *Appl. Phys. Lett.* **103** 194104
[9] Zhang S A, Xu S W, Ding J X, Lu C H, Jia T Q, Qiu J R and Sun Z R 2014 *Appl. Phys. Lett.* **104** 014101
[10] Yao Y, Zhang S, Zhang H, Ding J, Jia T, Qiu J and Sun Z 2015 *Sci. Rep.* **4** 07295
[11] Zhang H, Yao Y H, Zhang S A, Lu C H and Sun Z R 2016 *Chin. Phys.* B **25** 023201
[12] Zhang S A, Yao Y H et al 2015 *Sci. Rep.* **5** 13337
[13] Yao Y H, Cheng W J, Zheng Y, Xu C, Liu P, Jia T Q, Qiu J R, Sun Z R and Zhang S A 2017 *Laser Phys. Lett.* **14** 045301
[14] Wen F, Ali I, Hasan A, Li C B, Tang H J, Zhang Y F and Zhang Y P 2015 *Opt. Lett.* **40** 4599
[15] Ahmed N, Khan G A, Wang R M, Hou J R, Gong R, Yang L M and Zhang Y P 2017 *Opt. Lett.* **42** 1788
[16] Abdisa G, Ahmed I, Wang X X, Liu Z C, Wang H X and Zhang Y P 2016 *Phys. Rev.* A **94** 023849
[17] Li C B, Jiang Z H, Zhang Y Q, Zhang Z Y, Wen F, Chen H X, Zhang Y P and Xiao M 2017 *Phys. Rev. Appl.* **7** 014023
[18] Chuntonov L, Rybak L, Gandman A and Amitay Z 2008 *J. Phys. B: At. Mol. Opt. Phys.* **41** 35504
[19] Chuntonov L, Rybak L, Gandman A and Amitay Z 2008 *Phys. Rev.* A **77** 021403
[20] Chuntonov L, Rybak L, Gandman A and Amitay Z 2010 *Phys. Rev.* A **81** 045401